Science 322 (2008) 73 - 77

Surface-Modified Carbon Nanotubes Catalyze Oxidative Dehydrogenation of *n*-Butane

Jian Zhang, Xi Liu, Raoul Blume, Aihua Zhang, Robert Schlögl, Dang Sheng Su*

Fritz Haber Institute of the Max Planck Society, Faradayweg 4-6, D-14195 Berlin, Germany.

* To whom correspondence should be addressed. E-mail: dangsheng@fhi-berlin.mpg.de

Butenes and butadiene, which are useful intermediates for the synthesis of polymers and other compounds, are synthesized traditionally by oxidative dehydrogenation (ODH) of *n*-butane over complex metal oxides. Such catalysts require high O_2/butane ratios to maintain the activity, which leads to unwanted product oxidation. We show that carbon nanotubes with modified surface functionality efficiently catalyze the oxidative dehydrogenation of *n*-butane to butenes, especially butadiene. For low O_2/butane ratios, a high selectivity to alkenes was achieved for periods as long as 100 hours. This process is mildly catalyzed by ketonic C=O groups and occurs via a combination of parallel and sequential oxidation steps. A small amount of phosphorus greatly improved the selectivity by suppressing the combustion of hydrocarbons.

Transition metal oxides have been widely used as catalysts for the conversion of butane to C_4 alkenes, important industrial precursors for producing synthetic rubbers, plastics, and a number of industrially important chemicals. Despite a great deal of research, alkene selectivity in the current butane-to-butadiene process is severely limited (*1*). One important reason is that the unsaturated products are much more readily oxidized to CO_2 than is the starting alkane. The chemical complexity of polyvalent metal oxides, although found to be necessary for catalytic activity, impedes satisfactory selectivity through isolation of active sites (*2*–*6*). For this reason, the origin of the catalytic activity is debated, and there is as yet no generally accepted picture of the reaction mechanism (*7*, *8*).

Carbon materials have been reported to catalyze the oxidative dehydrogenation (ODH) of an aromatic molecule, ethylbenzene. However, conventional carbons, in particular activated carbon, underwent unavoidable deactivations due to coking or combustion (*9*–*12*). Recently, it was shown that only well-nanostructured carbons are stable and coke-free catalysts for styrene synthesis (*12*, *13*). Activation of C-H bonds in the ethyl group is considered to be coordinated by the ketonic carbonyl (C=O) group. Ethylbenzene has an aromatic moiety that enables relatively facile activation. Here, we report on surface-modified carbon nanotubes (CNTs) as a high-performance catalyst for the ODH of the much less active butane. Relative to metal-based catalysts, CNTs displayed an enhanced selectivity to C_4 alkenes, especially butadiene.

We conducted the reaction at 400° or 450°C with an O_2/butane ratio of 2.0. The product mixture contained only 1-butene, 2-butene, butadiene, CO_2, CO, and residual reactants; the resulting carbon balance was 100 ± 3% (fig. S1A) (*14*). In a blank experiment without catalyst, the alkene yield was as low as 0.9%. Over pristine CNTs, 88.9% of the converted butane was burnt, yielding 1.6% alkenes (Fig. 1A). Considering the intensive stability of CNTs in O_2 (fig. S1B) (*14*), we conclude that the CO_2 during the reaction mainly originated from the oxidation of the hydrocarbon feedstock and not from burning of the carbon catalysts. Neither washing CNTs in HCl solution nor loading with acidic nitro group could enhance the selectivity to alkene (fig. S2) (*14*).

We then functionalized surfaces of pristine CNTs with oxygen-containing groups by refluxing and oxidizing them in concentrated HNO_3 (*15*). With the resulting oCNTs as catalyst, we observed an improved yield of 6.7% alkenes. The alkene yield was further enhanced to 13.8% after the oCNTs catalyst was additionally modified by passivating defects with phosphorus [P-oCNTs, 0.5 ± 0.1 weight percent (wt %) P]. The increase in alkene selectivity is partially explained in Fig. 1B, which compares the catalytic performance of oCNTs and P-oCNTs for three individual reactions: (i) ODH of butane, (ii) ODH of 1-butene, and (iii) combustion of butadiene. The passivation apparently suppresses the activation and deep oxidation of the alkene substrates.

Preprint of the Department of Inorganic Chemistry, Fritz-Haber-Institute of the MPG *(for personal use only)* (www.fhi-berlin.mpg.de/ac)

A survey of recent literature showed that the P-oCNTs catalyst is as selective as the best V/MgO catalyst developed during the past 20 years (fig. S3A) (*14*). To compare the present reaction conditions to those previously used, we synthesized and evaluated two V/MgO samples. At the same conversion of butane, the $Mg_3V_2O_8$ and $Mg_3V_2O_7$ samples were less selective than P-oCNTs (fig. S3B) (*14*); in particular, relative to $Mg_3V_2O_7$, P-oCNTs gave twice the selectivity to butadiene (16.2%).

Safety can be a challenge when mixing hydrocarbons with oxidants. One solution is to operate the reaction under anaerobic conditions. After we reduced the O_2/butane ratio from 2.0 to 0.5, the P-oCNTs sample still exhibited outstanding stability. During a reaction lasting 100 hours, the butane and oxygen conversion remained almost unchanged, and the alkene selectivity stayed above 53% (Fig. 1C). To the best of our knowledge, the oxidative stability of P-oCNTs far exceeds those of metal oxide catalysts, which only work well with excess oxygen (O_2/butane ≥2), a condition necessary to prevent severe deactivation due to coke deposition.

In Fig. 1D, we show the ODH activity of oCNTs and P-oCNTs as a function of residence time. These results demonstrate that the overall reaction comprises a combination of parallel and sequential oxidation steps. The alkene selectivity at zero residence time was not unity (*16*), indicating that direct butane combustion occurred in parallel with the ODH reactions (i.e., butane to butenes, butane to butadiene). Two reaction pathways to butadiene were identified. Selectivity toward butadiene remained finite at the zero residence time, evidencing a primary ODH of butane to butadiene; it increased with the residence time as the selectivity of butenes deceased, revealing a secondary ODH of butenes to butadiene.

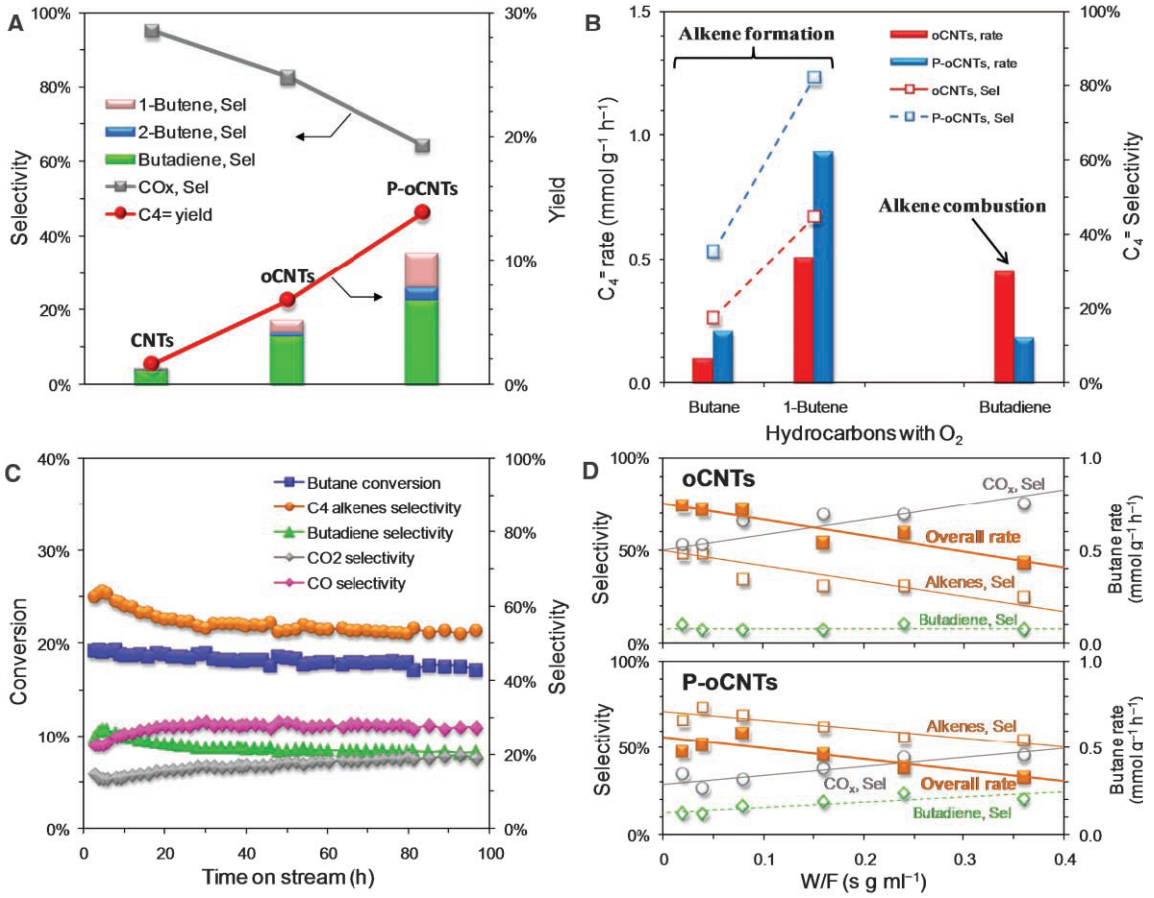

Fig. 1. ODH activities of various carbon nanotubes. (A) Performance of various CNTs for ODH of butane under oxygen-rich conditions: 0.18 g, 0.67% butane, O_2/butane = 2, 15 ml min^{-1}, 400°C. (B) Performance of modified CNTs in ODH reactions of butane and 1-butene and in combustion of butadiene: 0.18 g, 0.67% C_4 hydrocarbon, O2/butane = 2, 15 ml min^{-1}, 400°C. (C) Stability of P-oCNTs catalyst for ODH of butane over 100 hours: 0.18 g, 2.7% butane, O2/butane = 0.5, 10 ml min^{-1}, 450°C. (D) Dependence of product selectivity and reaction rate on residence time (W/F) in ODH reaction of butane: 0.005 to 0.09 g, 2.7% butane, O_2/butane = 0.5, 10 ml min^{-1}, 450°C. Helium was used as balance gas in all experiments.

Preprint of the Department of Inorganic Chemistry, Fritz-Haber-Institute of the MPG *(for personal use only)* (www.fhi-berlin.mpg.de/ac)

The effect of phosphorus as a promoter was studied by kinetic measurements. The initial rate constants for primary reactions were quantified as the residence time approached zero (*16*). After the modification with P, three important changes happened at the initial state: (i) The overall rate of converted butane decreased from 0.75 to 0.56 mmol g^{-1} $hour^{-1}$; (ii) the combustion of butane was reduced by as much as a factor of 2.3; and (iii) the formation rate of alkenes kept nearly unchanged at 0.38 to 0.40 mmol g^{-1} $hour^{-1}$. Therefore, P increased the selectivity by suppressing the combustion rate, rather than enhancing the formation rate of alkenes.

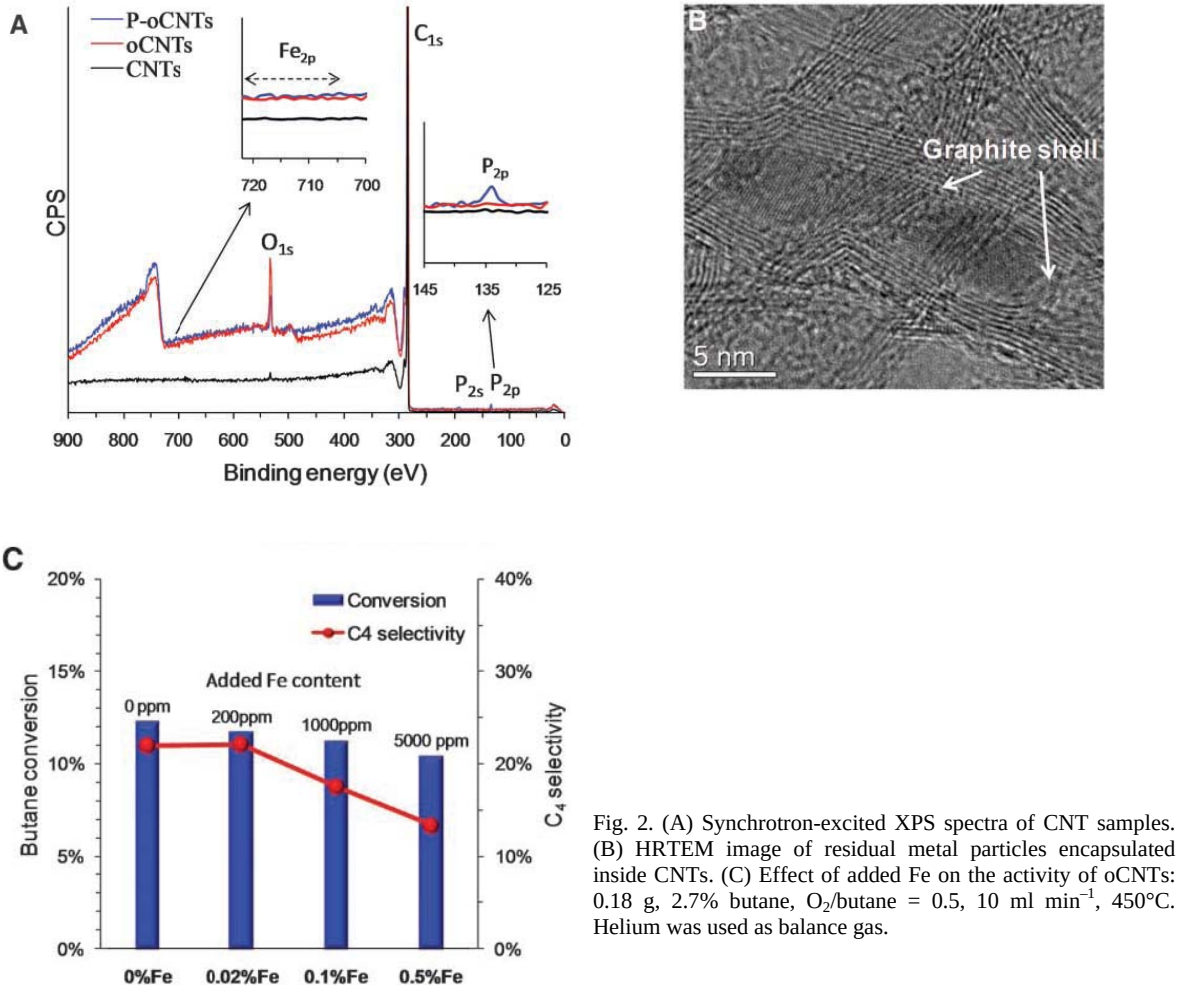

Fig. 2. (A) Synchrotron-excited XPS spectra of CNT samples. (B) HRTEM image of residual metal particles encapsulated inside CNTs. (C) Effect of added Fe on the activity of oCNTs: 0.18 g, 2.7% butane, O_2/butane = 0.5, 10 ml min^{-1}, 450°C. Helium was used as balance gas.

One of the key concerns in identifying and describing metal-free catalysis is the suspected influence of metal impurities in the catalyst. Commercial CNTs were prepared on supported metal catalysts, which inevitably remain as metal contaminants. Post-treatment by refluxing in strong acid effectively removed the residual metals to a great extent. X-ray fluorescence spectrometry revealed that the residual metals in the tested CNTs were very low (table S1) (*14*). The highest value of residual Fe was still as low as 0.09 wt %, as confirmed by energy-dispersive x-ray analysis (around 0.1 wt %). Furthermore, there was no signal of Fe or other metals in the surface layer at the limit of detection by synchrotron-excited x-ray photoelectron spectroscopy (XPS) (Fig. 2A). This difference suggests that if there is residual metal, it must be embedded in the carbon and not exposed to the reactants. This explanation is supported by the high-resolution transmission electron microscopy (HRTEM) image in Fig. 2B, which shows a catalyst particle encapsulated inside the CNTs. To fully exclude the role of Fe in the reaction, we deliberately added Fe to oCNTs in fractions ranging from 0.05 to 0.5 wt %. As shown in Fig. 2C, both the butane conversion and selectivity to C_4 alkenes gradually decreased with the increasing Fe content. Furthermore, there was no correlation of alkene selectivity with the residual metal content (fig. S4A) (*14*). We prepared a sample with 5% Fe phosphate in oCNTs; this sample also exhibited performance inferior to that of P-oCNTs without Fe (fig. S4B) (*14*). We can thus conclude that the reactivity originated exclusively from metal-free active sites on CNTs and that the residual metals played no positive role.

Preprint of the Department of Inorganic Chemistry, Fritz-Haber-Institute of the MPG *(for personal use only)* (www.fhi-berlin.mpg.de/ac)

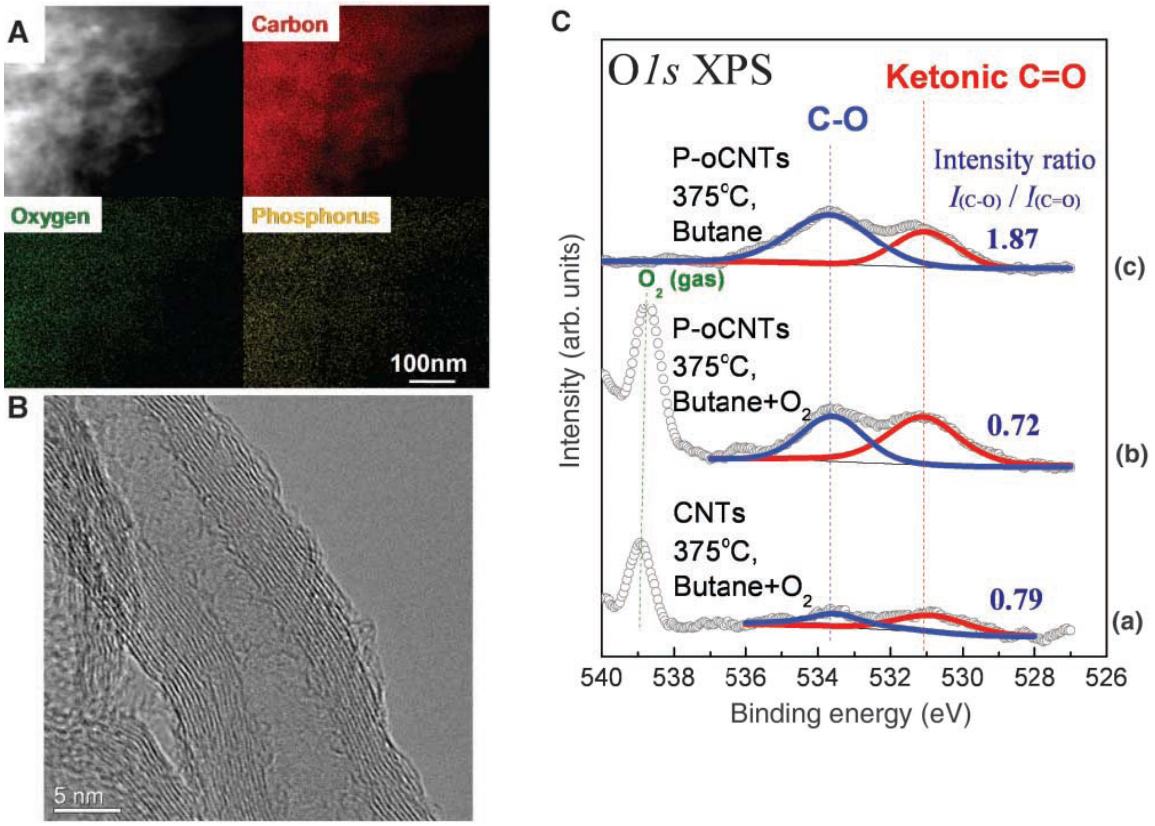

Fig. 3. (A) Elemental maps and (B) HRTEM image of the used P-oCNTs in Fig. 1A. (C) In situ O1s XPS spectra of working catalysts taken at 350° to 375°C: (a) CNTs: butane + O_2 (1:1), 0.25 mbar; (b) P-oCNTs: butane + O_2 (1:1), 0.25 mbar; (c) P-oCNTs: butane, 0.125 mbar.

To elucidate the structure-activity relation, we studied the morphological features by TEM with elemental mapping. Figure 3A gives an overview elemental map from a typical area. Both P and O are dispersed throughout the sample without aggregation. After an ODH reaction that ran for more than 800 min, the morphology of the CNTs remained intact and no evidence for their combustion was identified (Fig. 3B), as expected from the thermal stability data (fig. S1B) (*14*). Some areas of the outer and inner walls of the CNTs were covered by thin layers of phosphorus, which obviously differs from fullerenoid carbon species on pristine CNTs originating from condensation of hydrocarbon fragments (fig. S5) (*14*). Most of the surface of the CNTs did not give rise to carbon deposition, which is one advantage of this metal-free catalyst.

We also monitored the working surface of CNTs with near-ambient XPS (*17*). The best P-oCNTs catalyst was heated in vacuum to 350°C; at this temperature, the less stable groups (anhydride, carboxyl, ester, and nitro) would already have desorbed from the surface (fig. S6) (*14*). We identified two contributions from ketonic C=O groups (531.2 ± 0.2 eV) and from C- O groups (533.1 ± 0.2 eV) (i.e., ether and hydroxyl) (*15*, *18*). Relative amounts of C-O and C=O are represented in Fig. 3C by the ratio of their intensities, $I_{(C\text{-}O)}/I_{(C=O)}$. Under ODH conditions (butane + O_2, 1:1, 0.25 atm, 350° to 375°C), $I_{(C\text{-}O)}/I_{(C=O)}$.values ranged from 0.72 to 0.80. However, after switching off O_2, the $I_{(C\text{-}O)}/I_{(C=O)}$.value sharply increased to 1.87 (Fig. 3C) and the activity went to almost zero. This finding indicates that ketonic C=O groups are a critical ingredient of the active sites, whereas C-O groups constitute inactive intermediates or adsorbates.

Figure 4A summarizes our proposed mechanism for the CNTs-catalyzed butane oxidation. For this purpose, surface oxygen species are classified into electrophilic (superoxide O_2^-, peroxide O_2^{2-}) and nucleophilic (O^{2-}) types (*19*). Electrophilic oxygen species are electron-deficient and attack the electron-rich C=C bonds in alkenes, leading to the rupture of the carbon skeleton and subsequent combustion. Pristine CNTs were produced from chemical vapor deposition of unsaturated hydrocarbons, resulting in a number of structural defects and terminal carbon fragments. Below 600°C, these defect sites or edges of

Preprint of the Department of Inorganic Chemistry, Fritz-Haber-Institute of the MPG *(for personal use only)* (www.fhi-berlin.mpg.de/ac)

graphene have been reported to convert O_2 molecules to electrophilic oxygen species (*20*) and thus cause low selectivity to alkenes.

More controlled oxidation of carbon surfaces can be carried out in liquid-phase oxidants (*21*). After refluxing in HNO_3, defect sites were functionalized by O^{2-} anions into various functional groups. For example, ketonic C=O, a nucleophilic species with high electron density, preferentially reacts with electron-poor saturated bonds. However, at the reaction temperature, desorption of less stable groups results in new graphitic defects that subsequently generate new electrophilic oxygen sites, thus partially limiting the selectivity to alkenes on oCNTs. The addition of phosphate reacting with these defects suppresses the formation of electrophilic oxygen species (*22*). Thus, P-oCNTs displayed a lower overall activity but a much better selectivity.

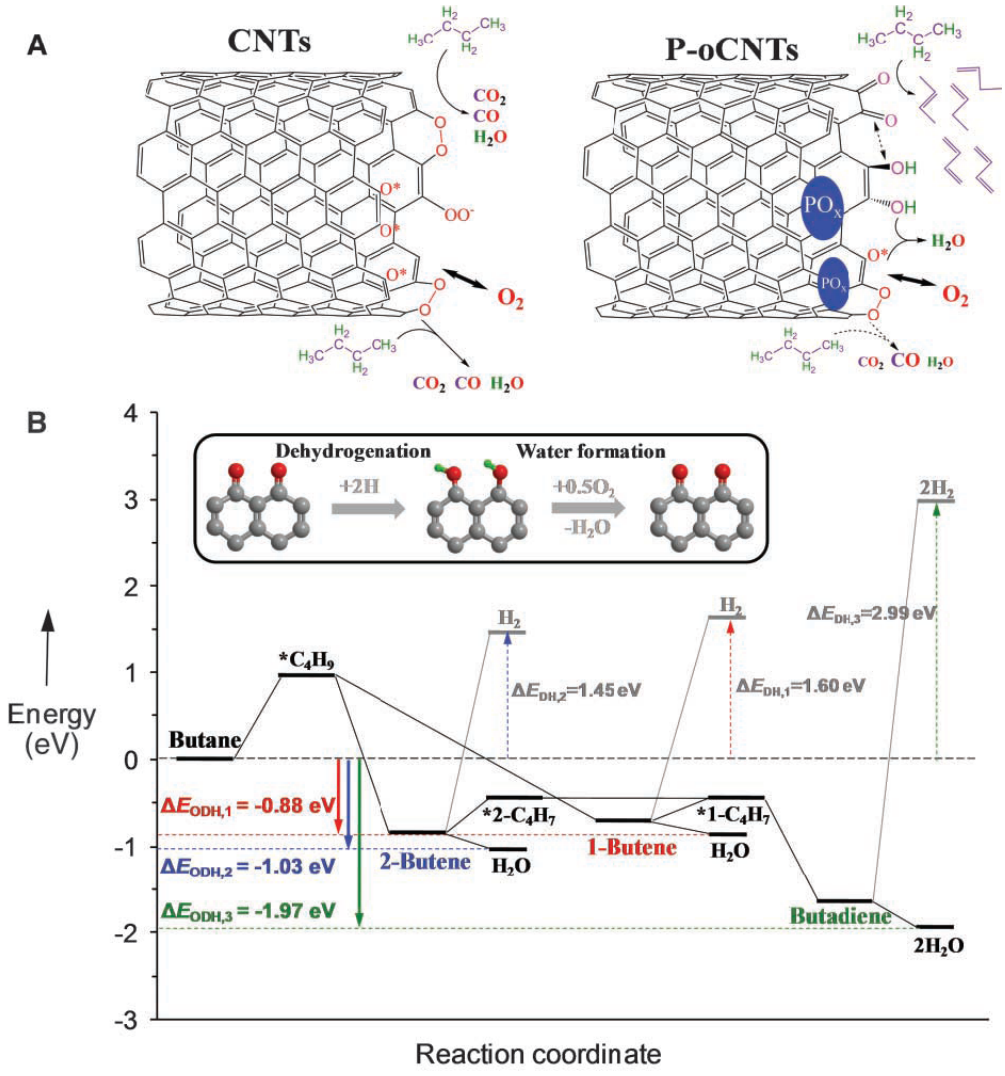

Fig. 4. (A) Schematic reaction and (B) energy steps of butane oxidation on pristine and P-modified CNTs.

We used density functional theory (DFT) calculations with the CASTEP code and the Perdew-Burke-Ernzerhof generalized gradient approximation (*23*, *24*) to study the ODH reaction over ketonic C=O groups. These calculations are independent of the precise mechanism and the transition state of each elementary step. We used the graphitic zigzag edge as a model to anchor the ketonic C=O groups (Fig. 4B). Conversion of butane is energetically controlled by the abstraction of the first H atom, which was predicted to be mildly endothermic at 0.92 eV. To convert butane into 1- or 2-butene, two C=O sites would ultimately be needed, and each one returns a single electron to the surrounding graphene as the reservoir. The remaining H atoms combine with surrounding oxygen to water, thereby closing the primary

Preprint of the Department of Inorganic Chemistry, Fritz-Haber-Institute of the MPG *(for personal use only)* (www.fhi-berlin.mpg.de/ac)

ODH cycle. The enthalpy of formation of water compensates for the endothermic dehydrogenation of butane. As a consequence, the calculated free energies for formation of 1- and 2-butenes were –0.88 eV and –1.03 eV, respectively. Another pathway to regenerate active sites is that H atoms recombine into H_2 molecules. However, as expected, such a direct dehydrogenation reaction is energetically unfavorable, because energy barriers are as high as 1.45 to 1.60 eV.

The DFT calculation also provides insights into the reaction pathways to butadiene. Butadiene may directly form from butane as primary product with an overall energy of –1.97 eV. However, the need for neighboring C=O sites to accommodate four H atoms in one elementary step does not seem to be pronounced, accounting for a much lower rate than the secondary ODH from butenes (Fig. 1D). It is more likely that C=O primarily activates butenes (rather than butane) to butadiene. The energy for the abstraction of the first H from butenes ($\Delta E_{\text{butenes,1H}}$), 0.25 to 0.40 eV, is much lower than that from butane ($\Delta E_{\text{butane,1H}}$), 0.92 eV. In this way, we can understand the influence of residence time. Because the residence time is long enough for the butenes produced to diffuse and react with the surrounding C=O sites, butadiene will be primarily generated from the secondary ODH, as demonstrated by the prevailing fraction of butadiene in C_4 alkenes in an integral reaction, 63 to 74% (Fig. 1A).

Our work contains some implications for catalysis in general. It is possible to imitate heterogeneously the concepts of homogeneous metal-free catalysis. The function of oxygen heteroatoms in molecular catalysts is reproduced by defects of bent graphitic sheets. The catalytic principle of site isolation can be realized by electronic localization of charges at the defect sites corresponding to molecular analogs of double bonds. The operation mode of ODH reactions can be studied on metal-free catalysts with greater precision than in metal oxide systems. There is neither lattice nor structural oxygen, but only oxygen at active sites. The present catalysts are free of polyvalent metal sites with complex electronic and spin structures, allowing for a facile theoretical treatment. Finally, the application of a heterogeneous CNTs catalyst is attractive because of favorable management of energy over a good thermal and electronic conductor.

References and Notes

1. F. Cavani, F. Trifirò, Appl. Catal. A 133, 219 (1995).
2. R. Grabowski, Catal. Rev. 48, 199 (2006).
3. K. D. Chen, A. T. Bell, E. Iglesia, J. Catal. 209, 35 (2002).
4. G. I. Panov, K. A. Dubkov, E. V. Starokon, Catal. Today 117, 148 (2006).
5. A. Miyakoshi, A. Ueno, M. Ichikawa, Appl. Catal. A 219, 249 (2001).
6. L. B.-Tapia, I. H. Pérez, P. Schacht, I. R. Córdova,
G. G. Aguilar-Ríos, J. Catal. 107–108, 371 (2005).
7. E. V. Kondratenko, M. Cherian, M. Baerns, Catal. Today 99, 59 (2005).
8. C. Resini, T. Montanari, G. Busca, J.-M. Jehng, I. E. Wachs, Catal. Today 99, 105 (2005).
9. T. G. Alkhazov, E. A. Ismailov, A. Yu, A. I. Kozharov, Kinet. Katal. 19, 611 (1978).
10. M. S. Kane, L. C. Kao, R. K. Mariwala, D. F. Hilscher, H. C. Foley, Ind. Eng. Chem. Res. 35, 3319 (1996).
11. M. F. R. Pereira, J. J. M. Órfão, J. L. Figueiredo, Appl. Catal. A 218, 307 (2001).
12. J. Zhang et al., Angew. Chem. Int. Ed. 46, 7319 (2007).
13. G. Mestl, N. I. Maksimova, N. Keller, V. V. Roddatis, R. Schlögl, Angew. Chem. Int. Ed. 40, 2066 (2001).
14. See supporting material on Science Online.
15. J.-H. Zhou et al., Carbon 9, 1379 (2007).
16. K. D. Chen, E. Iglesia, A. T. Bell, J. Phys. Chem. B 105, 646 (2001).
17. M. Salmeron, R. Schlögl, Surf. Sci. Rep. 63, 169 (2008).
18. T. I. T. Okpalugo, P. Papakonstantinou, H. Murphy, J. McLaughlin, N. M. D. Brown, Carbon 43, 153 (2005).
19. L. M. Madeira, M. F. Portela, Catal. Rev. 44, 247 (2002).
20. F. Atamny et al., Mol. Phys. 76, 851 (1992).
21. M. L. Toebes, J. M. P. van Heeswijk, J. H. Bitter, A. J. van Dillen, K. P. de Jong, Carbon 42, 307 (2004).
22. A. M. Puziy, O. I. Poddubnaya, A. M. Ziatdinov, Appl. Surf. Sci. 252, 8036 (2006).
23. S. J. Clark et al., Z. Kristallogr. 220, 567 (2005).
24. J. P. Perdew, K. Burke, M. Ernzerhof, Phys. Rev. Lett. 77, 3865 (1996).
25. We thank the Max Planck Society; U. Wild, A. Klein-Hoffmann, and J. Thielemann for technical assistance; Berliner Elektronenspeicherring-Gesellschaft für Synchrotronstrahlung for support of in situ XPS measurements; and M. A Smith for helpful discussions. Supported by the CANAPE project of the 6th Framework Programme of European Commission and the ENERCHEM project of the Max Planck Society.
Supporting Online Material www.sciencemag.org/cgi/content/full/322/5898/73/DC1

Preprint of the Department of Inorganic Chemistry, Fritz-Haber-Institute of the MPG *(for personal use only)* (www.fhi-berlin.mpg.de/ac)